https://doi.org/10.5194/egusphere-2026-2932
Preprint. Discussion started: 11 June 2026

Will there be more landslides and slushflows in Norway in a future climate?

Tuomo Saloranta[1], Graziella Devoli[1], Shaochun Huang[1], Wai K, Wong[1]

[1]Hydrology Department, Norwegian Water Resources and Energy Directorate (NVE), Oslo, N-0368, Norway

Correspondence to: Tuomo Saloranta (tus@nve.no)

Abstract.

Norway is exposed to mass movement type of natural hazards, such as landslides and slushflows, due to its steep terrain, wet climate, and long winter season. Understanding how these hazards may evolve under future climate conditions is essential for land-use planning and design of protective measures, among others. This study provides the first nationwide, quantitative assessment of how climate change may affect the hazard of landslides and slushflows in Norway, using operational hydrometeorological threshold models coupled to high-resolution climate and hydrological projections. These models are used to simulate daily landslide and slushflow hazard levels at 1×1 km resolution for both a reference period (1991–2020) and a future period (2071–2100) under a high greenhouse gas emission scenario. The results indicate a clear increase in landslide hazard across all regions of Norway. The frequency of moderate hazard levels (≥yellow) is projected to increase by 55–107 % depending on the region, mainly driven by increased water supply to the soil. In contrast, the response of slushflow hazard is strongly elevation-dependent. At lower elevations, reduced snow depth and shorter snow seasons lead to a decrease in slushflow hazard (−54 to −68 % depending on the region), while at higher elevations more liquid water supply cause a marked increase (+138 to +159 % depending on the region). Future research should focus on improving observational datasets and better evaluating the performance of hydrometeorological threshold models.

1 Introduction

Norway is exposed to frequent “mass movement” type of natural hazards (i.e. landslides, snow avalanches, rock falls, etc.) due to its steep mountainous terrain, relatively wet climate and long winter season. These natural hazards cause significant damage to transportation infrastructure and buildings as well as some casualties each year. These consequences and the efforts to mitigate them, through either structural or non-structural measures, are causing high costs to the Norwegian society.

Early warning systems (EWSs) are non-structural mitigation measures and exist for different natural hazards and for different types of mass movements, both at the regional and local scale in many countries (Stähli et al., 2015; Pecoraro et al., 2019; Guzzetti et al., 2020). Local EWSs aim to forecast the occurrence of a single or multiple mass movements on a specific slope (e.g. Pecoraro et al., 2019), while regional EWSs for mass movements are designed to forecast the hazard of

https://doi.org/10.5194/egusphere-2026-2932
Preprint. Discussion started: 11 June 2026

multiple mass movements that can impact wider geographic areas, such as districts, municipalities and cities. The daily forecasting of warning levels is usually based on a combination of output from numerical models and monitoring network (weather, hydrology, previous mass movement activity, etc.), some predefined thresholds and warning criteria as well as expert judgement (e.g. Piciullo et al., 2018; Guzzetti et al., 2020; Morin et al. 2020). In Norway, for example, EWSs for landslides, rock avalanches, snow avalanches and slushflows are operated by the Norwegian Water Resources and Energy Directorate (NVE) (Engeset et al., 2013; Krøgli et al., 2018; Kristensen et al., 2020; Sund et al., 2024). Daily hazard assessments are conducted by a group of forecasters and warnings are published at a common EWS website (www.varsom.no).

Some particular categories of mass movements, such as rockfalls and quick clay slides, are difficult to predict at regional scale due to the complicated physical or human activity related processes and slow response times connected to their triggering mechanisms. However, some other categories of mass movements, such as debris slides, debris avalanches, debris flows, snow avalanches and slushflows, have their main triggering mechanisms more closely related to the hydrological and meteorological drivers and the water cycle (e.g. to soil water content, precipitation intensity, accumulation and melt of the seasonal snow cover), which make them more predictable at regional level. These types of mass movements are here referred to as "weather-induced mass movements".

The ongoing global climate change is leading to a warmer and in many regions a wetter climate in the future (IPCC, 2021). Thus, besides the short-term advantages a society can gain from daily EWSs for weather-induced mass movements, there is also a longer-term challenge related to how the spatiotemporal patterns of weather-induced mass movements will change in the future due to changing climate. Such information on a decadal timescale is important in e.g. land-use planning and in prioritizing and correctly dimensioning the often costly long-term structural mitigation measures for e.g. landslides and snow avalanches. However, answers to the question of whether there will be more weather-induced mass movements in Norway in a future climate have so far been mostly based on subjective and qualitative expert opinions, as in Hanssen-Bauer et al. (2017) who foresaw an increase in landslides, wet snow avalanches and slushflows and a decrease in dry snow avalanches in a future climate. For some types of weather-induced mass movements there may be logical arguments to assume a generally increased occurrence in a warmer and wetter climate (Crozier, 2010; Gariano og Guzzetti, 2016). However, the causal relationships between changes in climate and in the occurrence of weather-induced mass movements are complicated since many different processes and triggering mechanisms, human activity included, may act simultaneously and be differently affected by climate change (Jakob, 2022; Stoffel et al., 2024; Gariano and Rianna, 2025). Counteracting processes can make it difficult to assess the net effect of climate change qualitatively by expert judgement only. For example, more rainfall and snow melt in a warmer and wetter climate could generally increase wet snow avalanche activity (Mitterer and Schweizer, 2013), but at the same time the shortening of the snow season length and reduced snow depths would generally reduce that. Similarly for landslides, the increased evapotranspiration in a warmer climate would alone contribute to drier soil conditions and thus reduced landslide activity, while the increased precipitation in a (warmer and) wetter climate would do the opposite (Crozier, 2010).

https://doi.org/10.5194/egusphere-2026-2932
Preprint. Discussion started: 11 June 2026

Gariano and Rianna (2025) reviewed 50 papers published in the period 1998–2023 dealing with the use of climate and landslide modelling chains in European study areas. Half of these studies predicted an increase in the frequency of landslides (mainly shallow), and one-third projected a reduction in the activity of more deep-seated movements. Most (45 out of 50) of these works were focused on a slope, regional or basin scale, while only three papers were focused on a national scale and two considered a transnational study area in central Europe. In Norway, no nationwide quantitative model-based studies on the climate change effects on weather-induced mass movement hazard have been published so far. Examples of more local scale studies in Norway include that by Melchiorre and Frattini (2012), who used precipitation projections with a coupled hydrology–slope stability model to simulate shallow landslide activity for the Otta area in eastern Norway, as well as the study by Oguz et al. (2024) who used present and future precipitation intensity-duration-frequency (IDF) estimates to simulate rainfall events for a physically based landslide model for the Stjørdal area in middle Norway. Melchiorre and Frattini (2012) did not find any conclusive trends while Oguz et al. (2024) reported an increase in landslide initiation probability.

For snow-related hazards, Eckert et al. (2024) reviewed studies of climate change impacts on snow avalanche activity and concluded that avalanche activity patterns will gradually shift from low to high elevations under continued warming. Mayer et al. (2024) simulated snow avalanche occurrences throughout the 21st century in the Swiss Alps using climate projections and a snow cover model, and found an overall decline in dry snow avalanche activity and an increase in wet snow avalanche activity. There are, however, very few published studies specifically of the climate change influence on slushflow hazard (i.e. the wettest type of snow avalanches; Eckert et al. 2024). Sidorova et al. (2011) found no or only slight changes in the area affected by slushflows in northern Europe, based on monthly average temperature and precipitation projections until 2050.

In this paper we use simple hydrometeorological threshold models, that are also applied operationally by the regional EWS for landslides in Norway (EWS-Ls-Nor), and simulate nationwide projections for the hazard of two important and frequently observed weather-induced mass movement types in a future climate, namely (i) landslides and (ii) slushflows (Fig. 1). The former type can be divided into many undercategories (Hungr et al. 2014), but our model encompasses basically debris avalanches, debris flows and debris slides, which are hereinafter collectively referred to as “landslides” in our paper. Landslides are usually triggered by high water input and/or instability in very wet debris (partly or fully water-saturated soil), leading to less friction and shallow rapid failures in the debris that slide or flow down steep slopes and/or channels (Hungr et al. 2014). Slushflows are mass movements of extremely water-soaked snow (slush) that are often confined to existing channels in the terrain, such as couloirs and creeks (Hestnes, 1998; Sund et al. 2024; Jædicke et al. 2024; Fig. 1). Slushflows often start in terrain depressions where water from intense rain and/or snow melt from a larger area is laterally drained into, immersing the snowpack locally and forming pools of slush (e.g. Blatny et al., 2026). Slushflows in snow-covered terrain bear some resemblance to debris flows, which is why they are included in the EWS-Ls-Nor instead of the snow avalanche EWS in Norway.

https://doi.org/10.5194/egusphere-2026-2932
Preprint. Discussion started: 11 June 2026

Figure 1: Examples of a landslide (left, northwestern Norway, photo: O. A. Jenssen, NVE) and a slushflow (right, northern Norway, photo: K. Hoseth, NVE).

Since landslides are usually weather-induced, their predictability is relatively high at regional level (Calvello et al., 2015; Devoli et al., 2021; Zhang et al., 2026). The review work by Gariano and Rianna (2025) highlighted the versatility of threshold models for landslides, that have been applied in studies of all spatial scales, ranging from the local slope to the wide transnational scale. These models can be derived empirically from statistical analysis of historical landslide episodes or from physically-based calculations (Guzzetti et al., 2008; Segoni et al., 2018). Most of them use a combination of rainfall intensity and duration as forcing, but also accumulated event rainfall and preceding rainfall conditions are used (Segoni et al., 2018). There are also examples of more multiparameter type of approaches, where several other variables are used in addition to rainfall to define hydrometeorological thresholds (Krøgli et al., 2018; Mirus et al., 2018; Marino et al., 2020; Palau et al., 2023). The approach used by EWS-Ls-Nor is an example of this, where simulated water input from rainfall and snowmelt to the ground, soil water content and landslide susceptibility are used in combination (see Sect. 3.3.1; Krøgli et al., 2018).

Similar simple hydrometeorological threshold models are in principle appropriate for snow avalanches too, but the complexity and importance of the continuously evolving weak layers within the snow pack (Schweizer et al., 2003) may often require the use of more detailed and complicated numerical snowpack models for prediction of snow avalanches (Morin et al. 2020). However, when a snow pack is thoroughly wetting and turning into slush, such weak layers are rapidly

https://doi.org/10.5194/egusphere-2026-2932
Preprint. Discussion started: 11 June 2026

destroyed and thus likely play a lesser role for triggering of slushflows than e.g. for wet snow avalanches (Baggi and Schweizer, 2009; Techel et al., 2011; D'Amboise et al., 2024). Consequently, hydrometeorological threshold models can be more readily applied for slushflows than for e.g. snow slab avalanches, as done in EWS-Ls-Nor (Sund et al., 2024; Sect. 3.3.2).

The methodology we apply in the following chapters to quantify the future consequences of climate change for landslides and slushflows in Norway is simple but quantitative and allows for model-based projections. Our study region is the mainland Norway, and the model chain in our study is the following: (1) an ensemble of bias-adjusted and downscaled climate model projections of temperature and precipitation (COR-BA-2025 data, Sect. 3.1) is used as forcing for the (2) distHBV hydrological model (Sect. 3.2), whose output provides the input for the (3) hydrometeorological threshold models for landslide and slushflow hazard prediction (Sect. 3.3). The outputs from this model chain are the landslide and slushflow hazard indicators with daily 1×1 km spatiotemporal resolution. Thus, the last element (3) in the model chain is for brevity referred to as "indicator models" in the following sections.

To our knowledge our study is the first model-based quantitative assessment of the climate change effects on landslide or slushflow hazards covering the entire Norway, and probably one of the few existing studies internationally that apply nationwide operational hydrometeorological threshold models for such projection purposes. Our model-based projections contribute to better and more reproducible and quantitative answers on the question whether there will be more landslides and slushflows in Norway in a future climate.

2 Study area

The Norwegian mainland covers an area of approximately 320 000 km^2, spans latitudes from 58 to 71° N and is predominantly mountainous terrain, with high relief and steep topography. Annual mean precipitation is highest (>2000 mm/yr) in the areas neighboring the Atlantic Ocean, while a drier more continental climate is found in the eastern and northeastern parts of the country (Dyrrdal et al., 2025). The winter season is generally longest in the northern Norway but snow is not uncommon in the lowland or southern parts of Norway either during the wintertime. The climate and the complex geological conditions make Norway prone to different types of mass movements, such as rockfalls, rock avalanches, rock slides, wet and dry snow avalanches, slushflows, debris flows, debris avalanches, debris slides, clay slides and quick clay slides.

The climate in Norway has become wetter and warmer in the recent decades. The annual average temperature over Norway has increased by 1° C from 1961-1990 to 1991-2020 and the precipitation has increased by 7 % in the same 30-year period (Dyrrdal et al., 2025). These general trends in temperature and precipitation are expected to continue towards the future with a projected further average warming of 3.4° C and increased precipitation by 11 % towards the end of this century (high emission scenario SSP3-7.0; Dyrrdal et al., 2025). The hydrometeorological consequences of a warmer and wetter climate are many, including a shorter snow season, less snow amounts, and more intense and frequent heavy precipitation episodes.

https://doi.org/10.5194/egusphere-2026-2932
Preprint. Discussion started: 11 June 2026

Although the spatial resolution is 1×1 km in our indicator model output (Sect. 3.3), we choose to aggregate and present our results for four different physiographic regions in Norway (Fig. 2) in order to reveal more robustly the large-scale geographical differences in the landslide and slushflow indicator model results. We use the same region division as in a previous historical landslide and slushflow indicator study by Saloranta et al. (2021). These four regions, differentiated by their geology, climate and geomorphological processes are described below.

1. Eastern Norway (81 000 km^2) contains extensive areas with forest, gentle valleys and rich arable land. The region is dominated by glacially scoured relatively low mountains and valleys, with steep slopes. Landslides of moderate size are typical in the valley areas, while large areas in this region also have low susceptibility to landslides. Slushflow activity is relatively low due to the more continental climate in this region.
2. Western Norway (71 000 km^2) is a mountainous region with alpine landscape or glacial relief characterized by deep valleys and fjords. The climate is generally maritime (mild and wet) and landslides and slushflows of moderate and large size are typical for this region.
3. Middle Norway (62 000 km^2) is comprised of gentle landscape with extensive lowland areas, rounded hills but also mountains with locally steep slopes. The climate is still maritime but less mild and wet as for Western Norway. Landslides and slushflows of moderate size are typical for this region.
4. Northern Norway (107 000 km^2) consists mostly of alpine landscape with deep valleys and steep slopes, but features also the large Finnmarksvidda plateau with an altitude mostly below 400 m in the northernmost interior part of the region. The climate in northern Norway is colder than in the other regions, but still rather maritime except for the easternmost parts. Landslides and slushflows of moderate and large size are typical for this region, except for Finnmarksvidda plateau which has a low susceptibility to landslides.

Figure 3 shows the frequency of observed landslide and slushflow incident days in eastern, western, middle and northern Norway in the period 2000-2025. Nearly 7000 registered landslide and slushflow observations from the period 2000-2025 are downloaded from the Norwegian mass movement database (NSDB; www.skredregistrering.no). The observations are not all strictly quality controlled, but in order to retain most of them the only filtering made was the removal of 334 observations due to unknown or too uncertain estimate of the incident time window (more than ± 9 days). The monthly distribution of incident days for landslides and slushflows varies clearly from region to region and shows a significant landslide activity throughout the year, while the main season for observed slushflows in Norway seems to be within December to May (Fig. 3). In the northern region, the frequency of slushflow incident days exceeds that of landslides during the winter months.

https://doi.org/10.5194/egusphere-2026-2932
Preprint. Discussion started: 11 June 2026

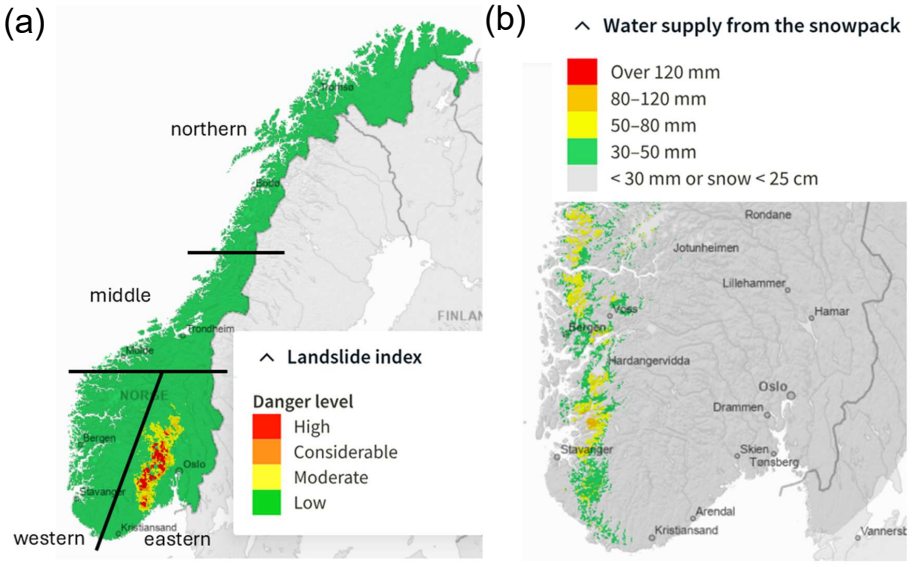

Figure 2: The four physiographic regions (black lines) used in our study, and examples of the daily (a) landslide and (b) slushflow indicator maps as they currently appear on the website www.senorge.no. The examples are from dates (a) 3 September 2024 and (b) 26 February 2026, displaying yellow, orange and red hazard levels in the eastern and western regions, respectively.

185

https://doi.org/10.5194/egusphere-2026-2932
Preprint. Discussion started: 11 June 2026

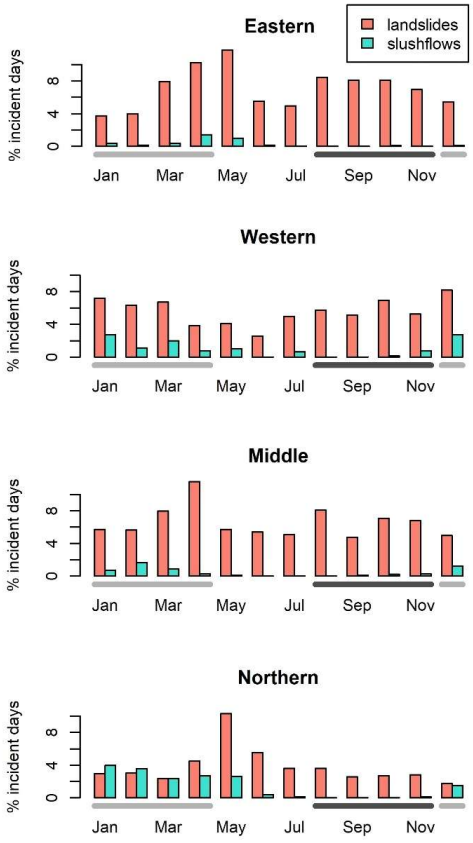

Figure 3: The mean fraction (%) of observed landslide (i.e. debris avalanches, -flows, and -slides) and slushflow incident days per month in eastern, western, middle and northern Norway in the period 2000-2025. The regions here are based on the 15 counties in Norway, but they roughly correspond to the climate analysis study regions shown in Fig. 2. An incident day is defined as a day when at least one landslide or slushflow observation is registered in the Norwegian mass movement database (NSDB). The thick horizontal lines below the x-axis denote the time windows used in our climate analysis of the landslide (black lines) and slushflow (grey lines) hazard indicators, respectively.

3 Data and methods

3.1 Bias-adjusted regional climate model projections (COR-BA-2025)

The first element in our model chain is the COR-BA-2025 ensemble of climate projections for Norway (Huang et al. 2025). This dataset was produced for the recent "Klima i Norge" ("Climate in Norway") assessment report (Dyrrdal et al., 2025)

https://doi.org/10.5194/egusphere-2026-2932
Preprint. Discussion started: 11 June 2026

and includes dynamically downscaled (1×1 km spatial resolution) and bias-adjusted regional climate model projections. The COR-BA-2025 ensemble dataset features 10 selected global/regional climate model combinations for Norway from a large ensemble of EURO-CORDEX simulation data archives, two bias-adjustment methods and three greenhouse gas emission scenarios: RCP2.6 (low), RCP4.5 (medium) and SSP3-7.0 (high) (Huang et al. 2025). We consider here the two bias-adjustment methods to give equally valid results (Huang et al. 2025) and select to include both of them in our ensemble of totally 20 projections per emission scenario. A description of the methods to generate COR-BA-2025 dataset are presented in more details in Huang et al. (2025).

In this paper we focus on the changes towards the end of century in the high emission scenario SSP3-7.0 featuring global climate models from the CMIP6 archives (wcrp-cmip.org). Similar indicator model results as presented in this paper, but for the middle of the century time-window (2041-2070) and for the low and medium emission scenarios are summarized in Appendix A8 in Dyrrdal et al. (2025). The high emission scenario is selected and presented here since it features the newest generation of available global climate models (CMIP6), and since it is the preferred precautionary scenario to be used in climate adaptation planning work in Norway (Dyrrdal et al. 2025).

3.2 Hydrological modelling

The hydrological projections for Norway, applied in our study, are generated by the distributed version of the HBV hydrological model (distHBV) (Beldring et al., 2003; Huang et al., 2025) using the COR-BA-2025 data (Sect. 3.1) as model forcing. The distHBV model runs at daily time steps for each 1×1 km grid cell in Norway. Each grid cell has one soil type but is divided into sub-grid tiles based on land cover information. The distHBV model mainly follows the model algorithms of the lumped HBV model (Bergström, 1995), but it applies the Penman-Monteith method to estimate potential evapotranspiration (PET) and calculates subgrid scale accumulation and ablation of snow, glacier ice melt, interception storage, distribution of soil moisture storage, evaporation, groundwater storage, runoff response, and lake evaporation (Huang et al., 2026). The results of processes are then aggregated by area weighting at the grid cell level.

Snowmelt is calculated by a simple degree-day method. Actual evapotranspiration (ET) from the soil layer is calculated based on a linear relationship between ET and PET and actual soil moisture for values below a certain fraction of field capacity, above which ET equals PET. Percolation from the soil moisture zone to the upper and lower groundwater zones is given as a nonlinear function of the soil moisture content, constant field capacity of the soil and the amount of water inflow to the soil moisture zone. Runoff is the sum of outflow from the upper and lower groundwater zones. The upper zone is a piecewise linear reservoir with a constant deep drainage to the lower zone. The lower zone is a linear reservoir, representing the slow outflow from catchment stores.

The distHBV model was calibrated against discharge measurements at 85 gauges from 2000 to 2007, and the long-term model performance was assessed by discharge measurements at 123 gauges from 1981 to 2014 (Huang et al., 2025). In the calibration period, about 50 % and 29 % of the catchments showed good and satisfactory results, respectively, and similar

https://doi.org/10.5194/egusphere-2026-2932
Preprint. Discussion started: 11 June 2026

model performance was also obtained for the 1981 to 2014 period, indicating a robust long-term model performance (Huang et al., 2025).

Based on the COR-BA-2025 climate projections (Sect. 3.1), distHBV generated in total 20 hydrological projections per greenhouse gas emission scenario from 1961/1971 to 2100/2098 depending on the global/regional climate model combinations. The four distHBV model output variables applied to calculate the landslide and slushflow hazard indicators (Sect. 3.3) were (1) snow water equivalent (*swe*) [mm], (2) water supply to the ground (*wou*) [mm/d], (3) soil moisture content (*hsm*) [mm] and (4) ground water storage (*hgw*) [mm].

3.3 Indicator models for landslide and slushflow hazard

The two indicator models applied in our study produce (i) the landslide hazard indicator called "HydMetGeo" (hereinafter referred to as the "HMG indicator") and (2) the slushflow hazard indicator called "Runoff from snowpack" (hereinafter referred to as the "RFS indicator"). These indicator models are simple and do not aim to include all possible triggering factors that could initiate a landslide or slushflow, but aim to include the most influential ones. Output from a hydrological model (distHBV in our study; Sect. 3.2) is required to provide the necessary variables for the calculation of these indicators, as explained below. The indicator models express their output value on a four-level hazard scale divided into green, yellow, orange and red levels. Daily maps of the HMG and RFS indicators are published at www.senorge.no (Fig. 2), both for the historical period back to 1957 and for the forecast period for the coming nine days. These maps are operationally used in the EWS-Ls-Nor aiding the forecasters in setting the correct daily regional landslide and slushflow warning levels.

3.3.1 The HMG indicator for landslide hazard

HMG indicator is the main indicator used for the assessment of the daily warning level for landslides in EWS-Ls-Nor. It uses as input (i) the relative water supply from rain and snow melt to the soil Q_{rel} [% of a 30-year annual mean value], (ii) the relative soil water content S_{rel} [% of a 30-year maximum value], and (iii) a susceptibility index which indicates how exposed the various areas in Norway are for landslides (Devoli et al., 2019).

The current operational HMG indicator in EWS-Ls-Nor (Krøgli et al., 2018) uses a combination of weights and threshold values to determine the hazard level classes. However, the algorithm can be approximated as a linear model of the type:

$$V_{HMG} = a + b \cdot Q_{rel} + c \cdot S_{rel} \quad (1)$$

where V_{HMG} is the dimensionless indicator value, a, b and c are the linear model parameters, Q_{rel} is derived from *wou* by dividing the current day's *wou* with a 30-year (1981-2010) average annual sum of *wou* for the same grid cell, and S_{rel} is derived similarly from (*hgw* + *hsm*) by dividing the current day's value with the maximum value registered in 1981-2010 for the same grid cell. The 1981-2010 reference period is the same as used for the operational HMG indicator in EWS-Ls-Nor (Krøgli et al. 2018).

https://doi.org/10.5194/egusphere-2026-2932
Preprint. Discussion started: 11 June 2026

In addition, three threshold values are needed to convert the value scale of V_{HMG} to a proposed HMG indicator class (green, yellow, orange and red levels, or alternatively classes 1-4). The current operational threshold values given in Krøgli et al. (2018) are used in our study. They are based on optimalization using a dataset of 206 recorded historical landslide events, as well as manual adjustments based on expert judgement. The final HMG indicator class value is determined as the minimum of the proposed HMG indicator class (1 to 4) and the susceptibility index class (also 1 to 4). For the susceptibility index data, we use the map by Devoli et al. (2019) which has the spatial resolution of first order catchments. Approximately 44 % of the land area of Norway is in this map defined as low (=1) susceptibility terrain, where consequently only the green HMG indicator hazard level (=1) occurrence is possible.

Factors that can be affecting the regional landslide hazard, but which are not included in the HMG indicator definition, are e.g. frozen soil conditions (often reducing the landslide hazard).

3.3.2 The RFS indicator for slushflow hazard

The RFS indicator we apply in our study is one of the two alternative indicators used in EWS-Ls-Nor for the daily assessment of the slushflow hazard. Another, more complicated slushflow indicator has been developed recently (Sund et al., 2024) and is in operational use, but it requires data on snowpack snow grain structure which are not available from our hydrological model runs.

The RFS indicator uses the liquid water (i.e. rain and snow melt) runoff from the bottom of the snow pack Q_s [mm/d] and (ii) snow depth H_s [cm] as input, where Q_s is equal to *wou* if there is snow (in snow free periods *wou* equals rainfall) and where H_s is derived from *swe* by assuming a constant snow density of 0.3 kg/L (i.e. $H_s = 0.1 \cdot swe/0.3$).

The threshold values for Q_s needed to define the hazard level classes are based on expert judgement. Same threshold values for Q_s are applied for all regions in Norway (green ≤50 mm/d, yellow >50 and ≤80 mm/d, orange >80 and ≤120 mm/d and red >120 mm/d). Moreover, if H_s is outside the preferential range for slushflows to occur (H_s range between 40 and 150 cm applied in our study) the RFS indicator is set to its lowest value (green hazard level). This corresponds to areas with too little snow to support significant slush formation or to areas where slush formation throughout the whole snow pack is considered to be limited due to the large snow amounts with higher liquid water absorption and retention capacity. Since no slushflow susceptibility map for Norway exists at the moment, the susceptibility index approach is not applied for the RFS indicator.

Factors that can be affecting the regional slushflow hazard, but which are not included in the RFS indicator definition, are e.g. (i) ground conditions below the snow pack, which affect water infiltration from the snow pack to the soil; (ii) the presence of snow- and ice-filled creek and couloir channels, which may clog waterways and enhance the mixing of channelized water flow with snow; (iii) a sudden water outburst when a lake is hit by a snow avalanche. Sund et al. (2024) argue in addition for a correlation between the snowpack snow grain structure and slushflow release, but the physical mechanisms behind this proposed effect remain largely undocumented and unexplained.

https://doi.org/10.5194/egusphere-2026-2932
Preprint. Discussion started: 11 June 2026

3.3.3 Spatiotemporal aggregation of results

In our analysis of the indicator model results we focus on the seasons where the HMG and RFS indicators are known to perform best and have the most relevance to predict the actual landslide or slushflow hazard levels. For the HMG indicator we focus on the four-month late summer and autumn season from 1. August to 30. November. This time-window excludes the season from December to July when frozen soil, prevailing snow melt and episodes of very local intense convective rainfall in the summertime may occur. For these specific conditions the HMG indicator is known to require extra interpretation by an experienced forecaster in order to avoid frequent false alarms or misses in capturing the actual landslide hazard level. The selected August-November time window covers 34-37 % of all the 530-675 observed incident days in 2000-2025 (Fig. 3), except in the northern region, where it covers 26 % of the 362 observed incident days.

For the RFS indicator we focus on the five-month main winter season from 1. December to 30. April. This time-window mostly excludes the main spring snow melt period and the prolonged snow melt period in the mountain areas when the RFS indicator is likely associated with more frequent false alarms. This is owing to the fact that the RFS indicator is not capturing the effect of a more established and effective water draining through the snow and snow-covered terrain, when many of the waterways (creeks and couloir channels) have become open and free from ice and snow, thus reducing the potential for water entrainment and accumulation in the snowpack and slush formation. The selected December-April time window covers 79-86 % of all the 43-136 observed incident days in 2000-2025 (Fig. 3), except in the eastern region, where it covers 66 % of the 29 observed incident days.

In our analysis, over the 30-year climatic normal periods 1991-2020 and 2071-2100, we sum up for each grid cell the number of daily occurrences of ≥yellow, ≥orange and red indicator levels. We thus use combined hazard levels, where e.g. the notation "≥yellow" corresponds to "at least yellow level" (i.e. including yellow, orange and red levels).

Spatiotemporally the indicators' occurrence counts are averaged over the four study regions (Sect. 2) and the selected 4-5 month time-windows. For the HMG indicator we exclude the highest grid cells with elevations over 1000 meters above sea level (m a.s.l.) in order to reduce the overestimation bias in the summer season, detected in Saloranta et al. (2021), due to high S_{rel} under the prevailing snow melt in the mountain areas.

4 Results

4.1 Projected changes in the hydrological variables from 1991-2020 to 2071-2100

Before analyzing the projection results for the landslide (HMG) and slushflow (RFS) indicators in a future climate, it is useful to first assess how their input variables, as simulated by the distHBV hydrological model, are projected to change. Table 1 shows the relative mean changes in Q_{rel}, S_{rel}, Q_s and H_s from the reference period (1991-2020) to the projected (2071-2100, high emission scenario) future climate in the four regions, while similar absolute mean changes with elevation are plotted in Fig. 4.

https://doi.org/10.5194/egusphere-2026-2932
Preprint. Discussion started: 11 June 2026

Table 1: Relative [%] mean changes from 1991-2020 to 2071-2100 in the input variables Q_{rel}, S_{rel}, Q_s and H_s for the HMG and RFS indicators in the four regions, as simulated by the distHBV model. Data for all the 20 projections in the model ensemble for the high greenhouse gas emission scenario SSP3-7.0 are used. For the HMG indicator input variables Q_{rel} and S_{rel} the mean is taken over all landslide-susceptible grid cells in the August-November season. For the RFS indicator input variables Q_s and H_s the mean is taken over the December-April season.

	ΔQ_{rel}	ΔS_{rel}	ΔQ_s	ΔH_s
Eastern	+19 %	+3 %	+35 %	−59 %
Western	+15 %	+2 %	+49 %	−43 %
Middle	+19 %	+3 %	+41 %	−59 %
Northern	+31 %	+1 %	+102 %	−50 %

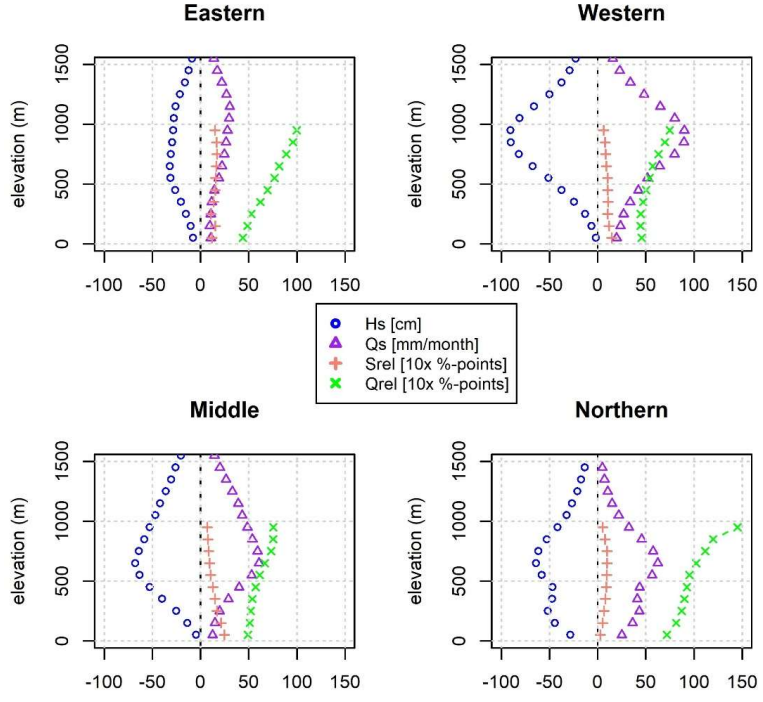

Figure 4: Mean absolute changes with elevation from 1991-2020 to 2071-2100 in the input variables Q_{rel}, S_{rel}, Q_s and H_s for the HMG and RFS indicators in the four regions, as simulated by the distHBV model. Data for all the 20 projections in the model ensemble for the high greenhouse gas emission scenario SSP3-7.0 are used. For the HMG indicator input variables Q_{rel} and S_{rel} the mean is taken over all landslide-susceptible grid cells in the August-November season. Their %-point units are for clarity multiplied by 10 in the figure (i.e. corresponding to "‰-points"). For the RFS indicator input variables Q_s and H_s the mean is taken over the December-April season.

https://doi.org/10.5194/egusphere-2026-2932
Preprint. Discussion started: 11 June 2026

Both Q_{rel} and Q_s show an increase towards the end of the century in all regions and in the two selected seasonal indicator time-windows. The relative change is largest for Q_s in the winter/spring season (35-102 % increase; Table 1) and much higher than the overall projected 10-12 % mean increase in total precipitation for all of Norway in winter and spring (Dyrrdal et al. 2025). Similarly also the change in Q_{rel} (15-31 % increase; Table 1) is somewhat higher than the overall projected 9-14 % mean increase in summer and autumn precipitation reported in Dyrrdal et al. (2025). The enhanced increases are likely due to contributions from more precipitation in form of rainfall than snowfall as well as from more snow melt during the winter/spring season in a future climate, not reflected in the total precipitation change numbers. The winter/spring increase in Q_s has a maximum at intermediate elevations between 500-1200 m a.s.l., while the late summer/autumn increase in Q_{rel} shows a rather steady increase with elevation between 0-1000 m a.s.l. (Fig. 4).

The snow depth H_s shows a decrease towards the end of the century in all regions (−43 to −59 % decrease; Table 1). The change in H_s with elevation is clearly negatively correlated with the increase in water supply Q_s in the winter/spring season (Fig. 4). The relative soil water content S_{rel} remains nearly unaltered in a future projected climate (1-3 % increase; Table 1).

4.2 Projected changes in the landslide and slushflow hazard indicators from 1991-2020 to 2071-2100

Figure 5 shows the cumulative distribution function (CDF) for the occurrences of HMG and RFS indicators per grid cell in the current and projected future climate in Norway. These results provide a useful insight into the typical return periods for the different indicator hazards levels. For the reference period (1991-2020) the CDF shows among others that in 11 % of Norway the ≥yellow hazard level in HMG indicator occurs more frequently than once per year, the ≥orange hazard level more frequently than once per 8 years and red level more frequently than once per 75 years (Fig. 5). Similarly for the RFS indicator, in 3 % of Norway the ≥yellow hazard level occurs more frequently than once per year, the ≥orange hazard level more frequently than once per 4 years and red level more frequently than once per 25 years (Fig. 5).

The projections towards the end of the century for the HMG indicator show more frequent occurrences of the ≥yellow, ≥orange and red hazard levels as compared to the reference period (Fig. 5). The area of Norway where the ≥yellow hazard level in HMG indicator occurs more frequently than once per year is increased by 16 %-points (from 11 to 27 %) in a projected future climate in 2071-2100, as compared to the reference period in 1991-2020. If only considering the landslide-susceptible area of Norway (56 % of total area) the increase is similarly 29 %-points.

For the RFS indicator the CDF in Fig. 5 shows no large changes from the reference to the future climate period for all of Norway on average. However, significant changes actually appear when considering different elevation levels, as revealed in Fig. 6 and 7.

https://doi.org/10.5194/egusphere-2026-2932
Preprint. Discussion started: 11 June 2026

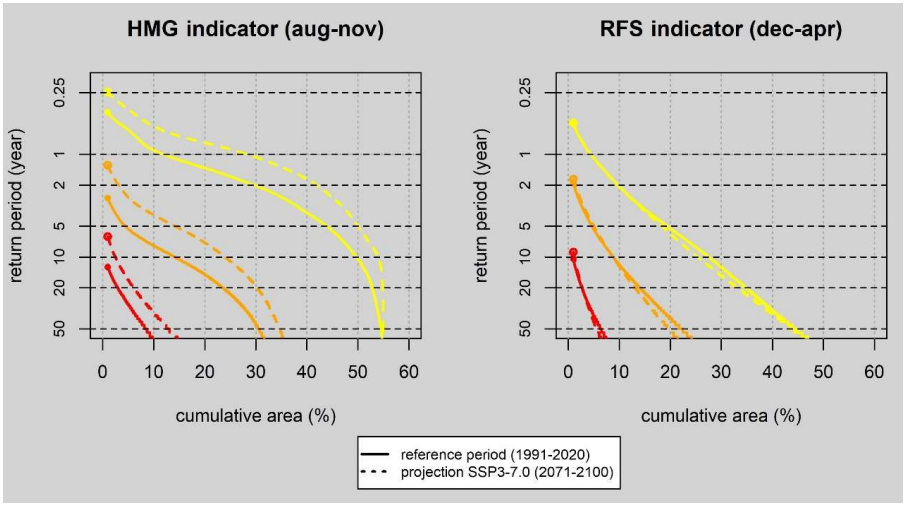

Figure 5: The cumulative distribution function of the mean HMG (left panel) and RFS (right panel) hazard indicator occurrences per grid cell in the reference (1991-2020; solid lines) and projected future (2071-2100; dashed lines) climate periods in Norway. Data for all the 20 projections in the model ensemble for the high greenhouse gas emission scenario SSP3-7.0 are used. The occurrence frequency is expressed as return period (years) on y-axis, while the x-axis shows the cumulative area (% of total land area in Norway). The line colors indicate the results for ≥yellow, ≥orange and red indicator levels. The lines start at 1 % cumulative area (filled circles). A version of this figure (in Norwegian) is published in Dyrrdal et al. (2025).

Figure 6 shows the elevation-wise mean occurrence of ≥yellow levels in HMG and RFS indicators in the four regions in the reference (1991-2020) and the future projection period (2071-2100). The general increase in HMG indicator from the reference to the future projection period is not very consistently dependent on the elevation. However, the projected change in RFS indicator shows a strong and consistent elevation dependency, where the peak of maximum indicator occurrence is shifted towards higher elevations in a future climate. The magnitude of this peak is only increased in the northern Norway region (Fig. 6).

While Fig. 6 shows results for the absolute values and ensemble means for the HMG and RFS indicators, the related elevation-wise changes from the reference (1991-2020) to the future projection period (2071-2100) for all the 20 ensemble members are shown in Fig. 7. The variability between the 20 ensemble members is considerable and indicates little consistent elevation dependency in the future changes in the HMG indicator (August-November), as pointed out above. The sign of this change (an increase) is the same for all regions and ensemble members (with one exception; Fig. 7). The mean projected increase in ≥yellow levels in the HMG indicator towards the end of century varies between regions (an increase by 0.23-0.43 d/yr, or by +55 to +107 %). A one-way ANOVA analysis of all the 20 projections in the model ensemble shows that only the HMG indicator increase in the eastern region (from 0.40 to 0.83 d/yr) is statistically significantly different from

https://doi.org/10.5194/egusphere-2026-2932
Preprint. Discussion started: 11 June 2026

the other regions at 5 % level of significance. Similar results for the higher ≥orange levels in HMG indicator (not shown) give a mean projected increase by 0.03-0.07 d/yr (+90 to +142 %) in the four regions towards the end of century.

For the RFS indicator (December-April) the elevation-wise pattern of change is very different from that of the HMG indicator. The mean change in ≥yellow level in the RFS indicator (Fig. 7) is clearly a decrease in indicator occurrence towards the end of the century below a certain elevation level, and an increase above that. This elevation level, where the sign of the change flips from a decrease to an increase, is hereinafter denoted as z_0 [m a.s.l.].

The eastern region shows on average a low RFS indicator occurrence, as compared to the other regions, and we thus omit this region in further analysis below. For the rest of the three regions (western, middle, northern), the ensemble mean value of the elevation z_0 decreases towards the north, from 780 m a.s.l. in the western region to 440 m a.s.l. in the northern region. Most of the 20 individual ensemble projections show the same elevation-dependent pattern of decrease and increase and a considerable spread on the magnitude of change and z_0 (Fig. 7). A one-way ANOVA analysis of all the 20 projections in the model ensemble shows that z_0 is statistically significantly different between these three regions at 5 % level of significance. The mean projected change in ≥yellow level occurrence in the RFS indicator towards the end of century shows a decrease by 0.08-0.36 d/yr (−54 to −68 %) below z_0 and an increase by 0.14-0.26 d/yr (+138 to +159 %) above z_0, depending on the region.

Results for the higher ≥orange level occurrence in the RFS indicator (not shown) reveal a similar elevation dependent pattern, where the ensemble mean value of the elevation z_0 decreases towards the north, from 780 m a.s.l. in the western region to 470 m a.s.l. in the northern region. The mean projected change in ≥orange level occurrence in the RFS indicator towards the end of century shows a decrease by 0.02-0.07 d/yr (−59 to −64 %) below z_0 and an increase by 0.03-0.05 d/yr (+124 to +164 %) above z_0.

https://doi.org/10.5194/egusphere-2026-2932
Preprint. Discussion started: 11 June 2026

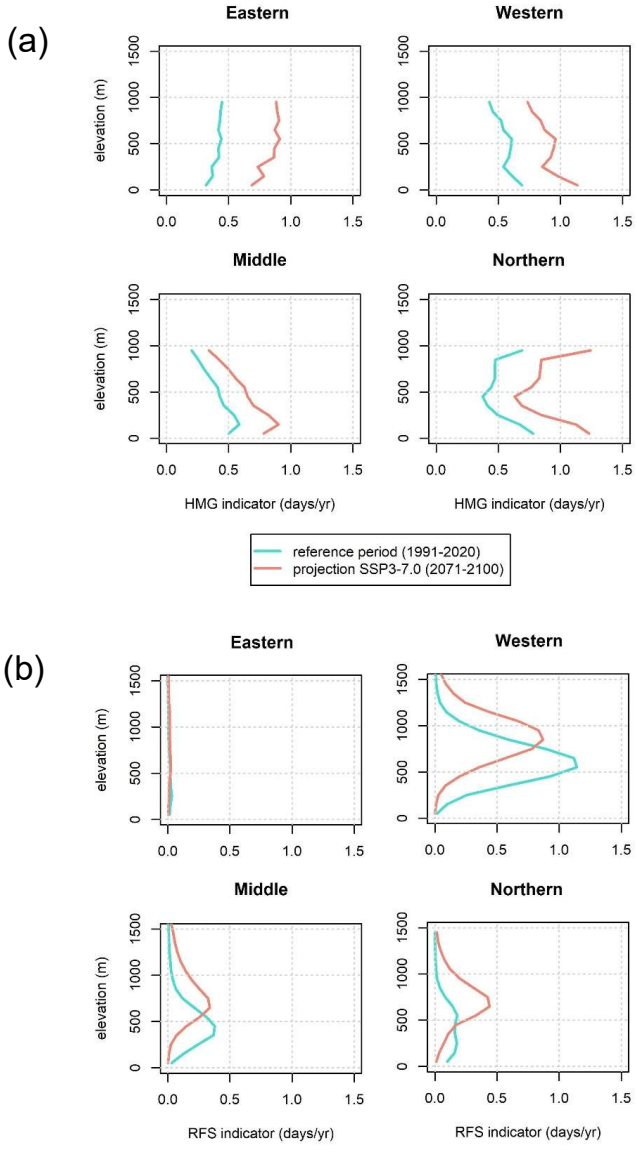

415 **Figure 6: Mean number of days per year with ≥yellow hazard level occurrence in (a) HMG (aug-nov) and (b) RFS (dec-apr) indicators at different elevations and regions in the reference period (1991-2020; blue lines) and projected (2071-2100; red lines) future climate. Data for all the 20 projections in the model ensemble for the high greenhouse gas emission scenario SSP3-7.0 are used.**

https://doi.org/10.5194/egusphere-2026-2932
Preprint. Discussion started: 11 June 2026

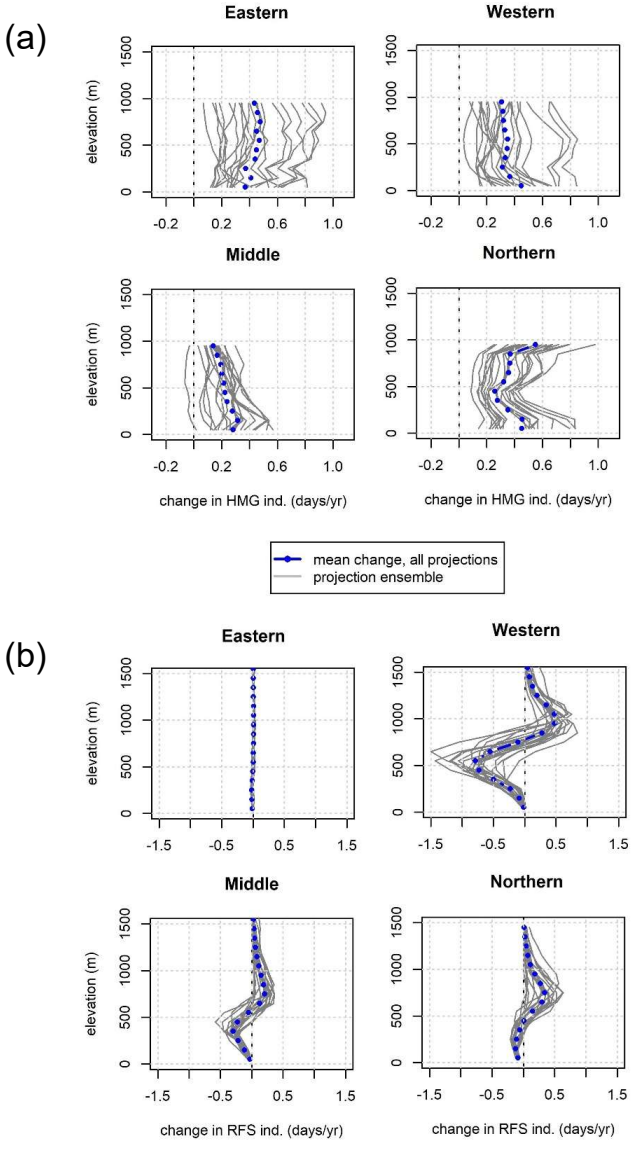

420 **Figure 7: The projected change from 1991-2020 to 2071-2100 in the mean number of days per year with ≥yellow hazard level occurrence in (a) HMG (aug-nov) and (b) RFS (dec-apr) indicators at different elevations and regions. The grey lines indicate the change for each of the 20 individual projections in the ensemble, while the pointed dark blue line shows the ensemble mean change.**

https://doi.org/10.5194/egusphere-2026-2932
Preprint. Discussion started: 11 June 2026

5 Discussion

The model-based projections for landslide and slushflow hazard indicators presented here can provide reproducible and quantitative answers to our research question on whether there will be more landslides and slushflows in Norway in a future climate. Numerical models, even simple ones, are often more capable than humans in synthesizing the varying effects and changes in the many, and sometimes counteracting, factors affecting the landslide and slushflow hazards. Thus, they can provide a strong alternative to more subjective and qualitative expert opinions on this important question (e.g. Hanssen-Bauer et al., 2017).

Our results of the projected changes in the hazard indicator occurrences show relatively large changes, both positive and negative, towards the end of century. For example, the range of mean relative changes mentioned in Sect. 4.2 for the HMG and RFS indicators (both ≥yellow and ≥orange hazard levels) vary from a decrease by 68 % to an increase by 164 %. These are larger in magnitude than one might first expect e.g. from a projected increase in precipitation by 11 % for Norway on average (Dyrrdal et al., 2025). The main reasons for the increase in HMG indicator occurrences towards the end of century are the increased water input to the soil and its intensity, leading to more indicator threshold-crossing days. The increased water input is not only due to more precipitation, but also due to increased number of days with precipitation as rain than snow and more snowmelt episodes in the late autumn. The relative soil water content, however, shows only minor changes in a projected future climate (Table 1; Fig. 4).

The increased HMG indicator occurrences towards the end of century in our results agree overall with the previous qualitative estimate of increased future landslide activity in Norway (Hanssen-Bauer et al., 2017), as well as with many of the studies on landslide-climate change relationships at different spatial scales in Europe, reviewed by Gariano and Rianna (2025). Half of the analyzed studies (25 out of 50) in their review foresaw a future increase in landslide activity, frequency or susceptibility. In most cases, these studies dealt with shallow landslides or debris, which is the scope also for our HMG indicator. The decreasing trends reported in one third (15 out of 50) of the reviewed studies in Gariano and Rianna (2025) were almost all related to deep-seated landslides, which are not relevant for the scope of the HMG indicator.

The conclusion from the local climate study for landslides in Norway by Melchiorre and Frattini (2012) was that, for Otta area in eastern Norway, large uncertainties in extreme rainfall projections, soil parameters, and antecedent soil moisture conditions hampered making reliable estimates of future changes in shallow landslide activity. Moreover, Saloranta et al. (2021) analyzed historical (1958–2020) time series of the same type of simulated hydrometeorological indicator maps for landslides and slushflows as in this paper over Norway. They found no statistically significant regional trends (at 5% level of significance) neither in the autumn landslide (September-November) nor in the winter/spring (November-June) slushflow indicators, and noted the high year-to-year variability and presence of counteracting forcing factors as explanations for the lack of significant trend estimates. Although our results also show large variability between the 20 different projections from the model ensemble (Fig. 7), a clear signal of change appears out of this extensive model ensemble on a regional scale, as discussed above. For another local area (Stjørdal) in middle Norway, the probabilistic method applied by Oguz et al. (2024)

https://doi.org/10.5194/egusphere-2026-2932
Preprint. Discussion started: 11 June 2026

for rainfall induced landslide occurrence predicted an increase in landslide initiation probability and landslide-susceptible areas under future climate conditions, agreeing with the general increase in HMG indicator occurrence in our results.

The elevation-wise pattern in the change of the RFS slushflow indicator occurrence towards a projected future climate is associated with the counteracting effects of (i) the generally increased water input to the snowpack (more precipitation, increased number of days with precipitation as rain than snow, and more meltwater from snowmelt episodes during the winter) and (ii) the shortening of the snow season and decreasing snow depths (Table 1; Fig. 4). As a net result the RFS indicator occurrence decreases on lower elevations (below z_0) and increases at higher elevations (above z_0) in a projected future climate. This two-fold pattern agrees with the results by Mayer et al. (2024) for wet snow avalanche activity, where they found a similar elevation-dependent pattern of change in their climate model study in the Swiss Alps. Similarly, Eckert et al. (2024) projected a migration of avalanche activity patterns from low to high elevations with an overall gradual decrease in activity, but with a transient state of increased activity that could exist at high elevations. Although the release mechanisms of slushflows and wet snow avalanches (Mitterer and Schweizer, 2013) differ in many ways, and are thus not directly comparable, they share the high liquid water flux to snowpack as a common triggering factor, and therefore such comparison of results is partly relevant.

When considering strictly slushflows only, Sidorova et al. (2011) reported no or only slight changes in the area affected by slushflows in northern Europe towards 2050. Our results reveal, on the contrary, a strong elevation dependency of the sign and amount of future change in slushflow occurrence. The likely decrease in slushflow activity at lower elevations, as shown by our results, was not foreseen in the previous qualitative estimate for Norway either (Hanssen-Bauer et al., 2017), where an overall increased future slushflow activity was anticipated. Eckert et al. (2024) noted that although a generalized increase in the frequency of slushflow events had not yet been proven, the occurrence of disrupting wet or slush-like events is likely to increase during peak winter conditions and at high elevations, agreeing broadly with our results. The elevation-wise increases and decreases in our RFS-indicator results seem, however, to cancel each other out on average on a larger spatial scale, leading to only small changes in a projected future climate when considering Norway as a whole (Fig. 5), agreeing in that way roughly with Sidorova et al. (2011).

Our study and results have been about indicators, that are used in operational forecasting in EWS-LS-Nor, and that can function as a proxy for real landslide and slushflow activity. The strength of this relationship (i.e. correlation between the indicators and observed landslide and slushflow incidents) needs, however, to be better quantified. One obstacle here is the lack of good quality observations on landslides and slushflows. The landslide and slushflow observations in the Norwegian mass movement database are mostly made in the vicinity of a road or other infrastructure and the size of the incident is not always numerically quantified and can vary from insignificantly small to disastrously large. In addition, some observations that are slushflows have probably been incorrectly registered as wet snow avalanches, and vice versa. In the future, landslides and slushflows may hopefully be more comprehensively mapped and counted by satellite imaging techniques, as described e.g. for snow avalanches by Eckerstorfer et al. (2017). Work is ongoing to quality control more mass movement observations and to better evaluate the performance of the hydrometeorological indicators against this data.

https://doi.org/10.5194/egusphere-2026-2932
Preprint. Discussion started: 11 June 2026

It is worth bearing in mind that the different elevation levels mentioned with our indicator results are related to the release areas of the landslides and slushflows and do not take into account the fact that the runout zones of these mass movements can reach significantly lower elevations, especially if the terrain is steep and/or the mass movement is of a large size or fluid type. Moreover, while the seasonal window applied for the RFS indicator covers most of the observed slushflow incident days, the time-window selected for the HMG indicator does not (Sect. 2). Consequently, our results do not apply for wintertime landslides (in areas where the soil is not frozen), or for summertime landslides which are often caused by very local and intense convective heavy rainfall episodes. The effects of more frequent and intense heavy rainfall episodes in the summer season, as well as less frozen ground conditions and more precipitation as rain than snow in the winter season in a future climate (Dyrrdal et al. 2025), will likely cause increased landslide occurrence also in the summer and winter seasons, respectively. Our analysis time-windows for the whole of Norway could in more regional applications be better customized to suit the characteristics of each region, as indicated in Fig. 3.

The changes in future landslide and slushflow activity projected here apply for large regions, seasonal time windows and for long-term decadal time periods, which should give more robust results than if studying more local or short-term changes. The relative changes in both the moderate (≥yellow) and more severe (≥orange) hazard level occurrence are approximately of similar sign and order of magnitude in our results (Sect. 4.2). It is worth remembering though, that long-term climatic trends may not eliminate the occurrence of very rare but high-impact episodes, which may be important to consider in hazard assessments and risk management, as pointed out by Peitzsch et al. (2026) for snow avalanche activity.

6 Conclusions

In this study we have applied simple hydrometeorological threshold models, used operationally by EWS-Ls-Nor, to simulate projections for landslide and slushflow hazard indicators over Norway towards year 2100 (high SSP3-7.0 greenhouse gas emission scenario). Our indicator models are forced with an ensemble of 20 hydrological projections from the distHBV hydrological model, that used the high-resolution (1×1 km) COR-BA-2025 bias-adjusted and downscaled climate model projections as its input forcing.

Our answer to the paper title and research question: “will there be more landslides and slushflows in Norway in a future climate?” is a “yes” for the landslide hazard, and a “yes and no” for the slushflow hazard, depending on the region and elevation level.

The HMG landslide hazard indicator occurrence (≥yellow level, August-November) projections show a significant increase in all of the four studied regions of Norway towards the end of century (on average a change by +0.23 to +0.43 d/yr, or by +55 to +107 %, depending on the region). These quantitative projections for the late summer/autumn season, as well as our qualitative assessments for the winter and summer seasons, suggest generally more landslide activity in a future climate.

The RFS slushflow hazard indicator occurrence (≥yellow level, December-April) shows also an increase (on average a change by +0.14 to +0.26 d/yr, or by +138 to +159 %) above 440-780 m a.s.l., depending on the region. However, below

https://doi.org/10.5194/egusphere-2026-2932
Preprint. Discussion started: 11 June 2026

these elevation levels, a mean decrease by −0.08 to −0.36 d/yr, or by −54 to −68 % is projected in a future climate. These projections suggest generally less slushflow activity on lower elevations and more activity higher up in the terrain in a future climate. In other words, the most active slushflow release areas seem to migrate to higher elevations towards the end of the century.

The overall regional future projected mean changes in the hazard indicator occurrences (≥yellow and ≥orange hazard levels for HMG and RFS indicators), ranging from a decrease by −68 % to an increase by +164 %, appear to be in relative terms larger in magnitude when compared e.g. to the projected increase in precipitation by 11 % for Norway on average (Dyrrdal et al., 2025). The model-related uncertainties and variability behind our mean results can readily be estimated from the set of 20 different projections in our model ensemble. This can be important information in e.g. project planning and cost-benefit analysis for structural mitigation measures for landslides and slushflows.

Data availability

The underlying research data is provided as a zip-file supplement to this paper. The zip-file contains 24 datafiles in semicolon-separated table format (.csv) as well as a README.pdf file explaining the content and structure of these tables in more details. The data included are: (i) observations of landslides and slushflows in 2000-2025 downloaded from the NSDB database; (ii) sum of indicator occurrences in each grid cell for the 20 different climate model and bias adjustment combinations in the ensemble, over the two 30-year periods and for the three different hazard levels; (iii) region, elevation and susceptibility index values for each grid cell; (iv) region- and elevation-wise mean values of the four input variables to the indicator models over the two 30-year periods and for the 20 different climate model and bias adjustment combinations in the ensemble.

Author contributions

TS designed the study and performed the indicator model computations and statistical analyses. GD contributed with expertise on landslide science and observational data. SH performed the hydrological model simulations and WKW performed the bias adjustment of climate model data. TS and all co-authors prepared the manuscript.

Competing interests

There are no conflicts of interest connected to this study.

https://doi.org/10.5194/egusphere-2026-2932
Preprint. Discussion started: 11 June 2026

Disclaimer

Copernicus Publications adds a standard disclaimer: "Copernicus Publications remains neutral with regard to jurisdictional claims made in the text, published maps, institutional affiliations, or any other geographical representation in this paper. While Copernicus Publications makes every effort to include appropriate place names, the final responsibility lies with the authors. Views expressed in the text are those of the authors and do not necessarily reflect the views of the publisher."
Please feel free to add disclaimer text at your choice, if applicable.

Acknowledgements

We acknowledge the World Climate Research Programme, the CORDEX Science Advisory Team (SAT) - coordinating body of CORDEX, and the Working Group on Coupled Modelling (WGCM) - responsible panel for CMIP6. We thank the different CORDEX climate modeling groups for producing and making available their model output, CMIP6 for providing the driving data, the Earth System Grid Federation (ESGF) for providing access, and the multiple funding agencies who support CORDEX, CMIP and ESGF. This work was done as part of the research project nr. 80540 at Norwegian Water Resources and Energy Directorate (NVE).

Review statement

The review statement will be added by Copernicus Publications listing the handling editor as well as all contributing referees according to their status anonymous or identified.

References

Baggi, S. and Schweizer, J.: Characteristics of wet-snow avalanche activity: 20 years of observations from a high alpine valley (Dischma, Switzerland), Nat Hazards, 50, 97–108, https://doi.org/10.1007/s11069-008-9322-7, 2009.

Beldring, S., Engeland, K., Roald, L. A., Sælthun, N. R., and Voksø, A.: Estimation of parameters in a distributed precipitation-runoff model for Norway, Hydrol. Earth Syst. Sci., 7, 304–316, https://doi.org/10.5194/hess-7-304-2003, 2003.

Bergström, S.: The HBV model, in: Computer models of watershed hydrology. edited by: Singh, V. P., Water Resources Publications, 443-476, ISBN 978-1-887201-74-2, 1995.

Blatny, L., Hamre, D., Gaume, J., Gauer, P. and Mears, A.: Observations and modeling of slushflows from Atigun Pass, Alaska, Cold Regions Science and Technology, 245, 104812, https://doi.org/10.1016/j.coldregions.2025.104812, 2026.

https://doi.org/10.5194/egusphere-2026-2932
Preprint. Discussion started: 11 June 2026

Calvello, M., d'Orsi, R. N., Piciullo, L., Paes, N., Magalhaes, M. and Lacerda, W. A.: The Rio de Janeiro early warning system for rainfall-induced landslides: analysis of performance for the years 2010–2013, Int. J. Disaster Risk Reduct., 12, 3-15, https://doi.org/10.1016/j.ijdrr.2014.10.005, 2015.

Crozier, M. J.: Deciphering the effect of climate change on landslide activity: A review, Geomorphology, 124, 260–267, https://doi.org/10.1016/j.geomorph.2010.04.009, 2010.

D'Amboise, C., Hansen, V., Hendrikx, J. and Vick, L.: Motivation for slushflow classification, in: Proceedings of the International Snow Science Workshop, 23-27 Sept 2024, Tromsø, Norway, 759-765, https://arc.lib.montana.edu/snow-science/objects/ISSW2024_P6.4.pdf, 2024.

Devoli, G., Bell, R. and Cepeda, J.: Susceptibility map at catchment level, to be used in landslide forecasting, Norway, NVE-rapport 2019:1, Norges vassdrags- og energidirektorat (NVE), Oslo, Norway, https://publikasjoner.nve.no/rapport/2019/rapport2019_01.pdf, 2019.

Devoli, G., Colleuille, H., Sund, M. and Wasrud, J.: Seven years of landslide forecasting in Norway—strengths and limitations, in: Understanding and reducing landslide disaster risk, edited by: Casagli, N., Tofani, V., Sassa, K., Bobrowsky, P. T. and Takara, K., Springer, https://doi.org/10.1007/978-3-030-60311-3_30, 2021.

Dyrrdal, A. V., Bakke, S. J., Hanssen-Bauer, I., Mayer, S., Nilsen, I. B., Nilsen, J. E. Ø., Paasche, Ø., Saloranta, T. and Årthun, M. (Eds.): Klima i Norge – kunnskapsgrunnlag for klimatilpasning oppdatert i 2025, NCCS-rapport 1/2025, https://doi.org/10.60839/4rgq-nn84, 2025.

Eckerstorfer, M., Malnes, E. and Müller. K.: A complete snow avalanche activity record from a Norwegian forecasting region using Sentinel-1 satellite-radar data, Cold Regions Science and Technology, 144, 39-51, https://doi.org/10.1016/j.coldregions.2017.08.004, 2017.

Eckert, N., Corona, C., Giacona, F., Gaume, J., Mayer, S., van Herwijnen, A., Hagenmuller, P. and Stoffel, M.: Climate change impacts on snow avalanche activity and related risks, Nat. Rev. Earth Environ., 5, 369–389, https://doi.org/10.1038/s43017-024-00540-2, 2024.

Engeset, R. V.: National Avalanche Warning Service for Norway – established 2013, in: Proceedings of the International Snow Science Workshop, 7–11 October 2013, Grenoble, France, 301–310, https://arc.lib.montana.edu/snow-science/objects/ISSW13_paper_P1-19.pdf, 2013.

Gariano, S. L. and Guzzetti, F.: Landslides in a changing climate, Earth-Science Reviews, 162, 227–252, https://doi.org/10.1016/j.earscirev.2016.08.011, 2016

Gariano S. L. and Rianna G.: How will the projected climate change influence rainfall induced landslides in Europe? A review of modelling approaches, Landslides, 22, 3011–3027, https://doi.org/10.1007/s10346-025-02550-7, 2025.

https://doi.org/10.5194/egusphere-2026-2932
Preprint. Discussion started: 11 June 2026

Guzzetti, F., Peruccacci, S., Rossi, M and Stark, C. P.: The rainfall intensity–duration control of shallow landslides and debris flows: an update, Landslides 5, 3–17, https://doi.org/10.1007/s10346-007-0112-1, 2008.

Guzzetti F., Gariano S., Peruccacci S., Brunetti M.T., Marchesini I., Rossi M., Melillo M.: Geographical landslide early warning systems, Earth-Science Reviews, 200, 102973, https://doi.org/10.1016/j.earscirev.2019.102973, 2020.

Hanssen-Bauer, I., Førland, E. J., Haddeland, I., Hisdal, H., Lawrence, D., Mayer, S., Nesje, A., Nilsen, J. E. Ø., Sandven, S., Sandø, A. B., Sorteberg, A. and Ådlandsvik, B. (Eds.): Climate in Norway 2100 – a knowledge base for climate adaptation, report 1-2017, Norwegian Centre for Climate Services (NCCS), https://www.met.no/kss/_/attachment/download/e1d26477-1c7c-4912-8af9-a2b20a0c084f:c615e5a9799582b64d52542878edf0d607d515dc/klimarapport-2100-engelsk-web-0160517.pdf, 2017.

Hestnes E. Slushflow hazard — where, why and when? 25 years of experience with slushflow consulting and research, Annals of Glaciology, 26, 370-376, https://doi.org/10.3189/1998AoG26-1-370-376, 1998.

Huang, S., Wong, W. K., Dobler, A., Bakke, S. J., Beldring, S., Haddeland, I., Hygen, H. O., Løvset, T., Mayer, S., Melvold, K., Nilsen, I. B., Ruan, G., Sørland, S. L., and Dyrrdal, A. V.: An improved modelling chain for bias-adjusted high-resolution climate and hydrological projections for Norway, EGUsphere [preprint], https://doi.org/10.5194/egusphere-2025-5331, 2025.

Huang, S., Wong, W. K., Tveito, O. E. and Haddeland, I.: Impacts of empirical and physical evaporation methods on changes in hydrological components and drought indices under climate change scenarios, Hydrology Research, 57, 765–784, https://doi.org/10.2166/nh.2026.220, 2026.

Hungr, O., Leroueil, S. and Picarelli, L.: The Varnes classification of landslide types, an update, Landslides, 11, 167–194, https://doi.org/10.1007/s10346-013-0436-y, 2014.

IPCC, 2021: Climate change 2021: the physical science basis, Contribution of Working Group I to the Sixth Assessment Report [Masson-Delmotte, V., et al. (eds.)], Cambridge University Press, 2391 pp., https://doi.org/10.1017/9781009157896, 2021.

Jaedicke, C., Sund, M., Grímsdóttir, H., Helgason, J. K., Bartsch, U. B. A., Sandersen, F., and Morken, E.: Classification of slushflow release areas in Norway and Iceland, in: Proceedings of the International Snow Science Workshop, 23-27 Sept 2024, Tromsø, Norway, 785-791, https://arc.lib.montana.edu/snow-science/objects/ISSW2024_P6.9.pdf, 2024.

Jakob, M.: Landslides in a changing climate, in: Landslide hazards, risks, and disasters, edited by: Tim Davies, Nick Rosser, J.F. Shroder (Eds.), Landslide Hazards, Risks, and Disasters, 505-579, Elsevier, https://doi.org/10.1016/B978-0-12-818464-6.00003-2, 2022

https://doi.org/10.5194/egusphere-2026-2932
Preprint. Discussion started: 11 June 2026

Kristensen L., Pless G., Blikra L. H. and Anda E.: Management and monitoring of large rockslides in Norway, in: Proceedings of the ISRM International Symposium - EUROCK 2020, physical event not held, 14 June 2020, paper nr. 005, https://onepetro.org/ISRMEUROCK/proceedings-abstract/EUROCK20/EUROCK20/ISRM-EUROCK-2020-005/447322?redirectedFrom=PDF, 2020.

Krøgli, I. K., Devoli, G., Colleuille, H., Boje, S., Sund, M., and Engen, I. K.: The Norwegian forecasting and warning service for rainfall- and snowmelt-induced landslides, Nat. Hazards Earth Syst. Sci., 18, 1427–1450, https://doi.org/10.5194/nhess-18-1427-2018, 2018.

Marino, P., Peres, D. J., Cancelliere, A., Greco, R. and Bogaard T. A.: Soil moisture information can improve shallow landslide forecasting using the hydrometeorological threshold approach, Landslides, 17, 2041–2054, https://doi.org/10.1007/s10346-020-01420-8, 2020.

Mayer, S., Hendrick, M., Michel, A., Richter, B., Schweizer, J., Wernli, H., and van Herwijnen, A.: Impact of climate change on snow avalanche activity in the Swiss Alps, Cryosphere, 18, 5495–5517, https://doi.org/10.5194/tc-18-5495-2024, 2024.

Melchiorre, C. and Frattini, P.: Modelling probability of rainfall-induced shallow landslides in a changing climate, Otta, Central Norway, Climatic Change, 113, 413–436, https://doi.org/10.1007/s10584-011-0325-0, 2012.

Mirus, B. B., Morphew, M. D. and Smith, J. B.: Developing hydro-meteorological thresholds for shallow landslide initiation and early warning, Water, 10, 1274, https://doi.org/10.3390/w10091274, 2018.

Mitterer, C. and Schweizer, J.: Analysis of the snow-atmosphere energy balance during wet-snow instabilities and implications for avalanche prediction, The Cryosphere, 7, 205–216, https://doi.org/10.5194/tc-7-205-2013, 2013.

Morin, S., Horton, S., Techel, F., Bavay, M., Coléou, C., Fierz, C. Gobiet, A., Hagenmuller, P., Lafaysse, M., Ližar, M., Mitterer, C., Monti, F., Müller, K., Olefs, M., Snook, J. S., van Herwijnen, A. and Vionnet, V.: Application of physical snowpack models in support of operational avalanche hazard forecasting: A status report on current implementations and prospects for the future, Cold Regions Science and Technology, 170, 102910, https://doi.org/10.1016/j.coldregions.2019.102910, 2020.

Oguz, E. A., Benestad, R. E., Parding, K. M., Depina, I., and Thakur, V.: Quantification of climate change impact on rainfall-induced shallow landslide susceptibility: a case study in central Norway, Georisk: Assessment and Management of Risk for Engineered Systems and Geohazards, 18, 467–490, https://doi.org/10.1080/17499518.2023.2283848, 2024.

Palau, R. M., Berenguer, M., Hürlimann, M. and Sempere-Torres, D.: Implementation of hydrometeorological thresholds for regional landslide warning in Catalonia (NE Spain), Landslides, 20, 2039–2054, https://doi.org/10.1007/s10346-023-02094-8, 2023.

https://doi.org/10.5194/egusphere-2026-2932
Preprint. Discussion started: 11 June 2026

Pecoraro, G., Calvello, M. and Piciullo, L: Monitoring strategies for local landslide early warning systems, Landslides, 16, 213–231, https://doi.org/10.1007/s10346-018-1068-z, 2019.

Peitzsch, E. H., Martin, J. T., Greene, E. M., Eckert, N., Favillier, A., Konigsberg, J., Kichas, N., Stahle, D. K., Birkeland, K. W., Elder, K., and Pederson, G. T.: Changing drivers of regional large magnitude avalanche frequency throughout Colorado, USA, Nat. Hazards Earth Syst. Sci., 26, 1059–1074, https://doi.org/10.5194/nhess-26-1059-2026, 2026.

Piciullo, L., Calvello, M. and Cepeda, J.M.: Territorial early warning systems for rainfall-induced landslides, Earth-Sci. Rev., 179, 228–247, https://doi.org/10.1016/j.earscirev.2018.02.013, 2018.

Saloranta, T., Colleuille, H. and Andersen J.: Analyse av variabilitet og trender (1958-2020) i skredfareindekser brukt i NVEs jord-, sørpe- og flomskredvarslingstjeneste, NVE-rapport 2021:24, Norges vassdrags- og energidirektorat (NVE), Oslo, Norway, https://publikasjoner.nve.no/rapport/2021/rapport2021_24.pdf, 2021.

Schweizer, J., Jamieson, J. B. and Schneebeli, M.: Snow avalanche formation, Rev. Geophys., 41, 1016, https://doi.org/10.1029/2002RG000123, 2003.

Segoni, S., Piciullo, L. and Gariano S. L.: A review of the recent literature on rainfall thresholds for landslide occurrence, Landslides, 15, 1483–1501, https://doi.org/10.1007/s10346-018-0966-4, 2018.

Sidorova T, Belaya N, Perov V.: Distribution of slushflows in northern Europe and their potential change due to global warming, Annals of Glaciology, 32, 237-240, https://doi.org/10.3189/172756401781819742, 2001.

Stoffel, M., Allen, S.K., Ballesteros-Cánovas, J.A., Jakob, M., and Oakley, N.: Climate Change Effects on Debris Flows, in: Advances in debris-flow science and practice, edited by: Jakob, M., McDougall, S. and Santi, P., Springer, 273–308, https://doi.org/10.1007/978-3-031-48691-3_10, 2024.

Stähli, M., Sättele, M., Huggel, C., McArdell, B. W., Lehmann, P., Van Herwijnen, A., Berne, A., Schleiss, M., Ferrari, A., Kos, A., Or, D., and Springman, S. M.: Monitoring and prediction in early warning systems for rapid mass movements, Nat. Hazards Earth Syst. Sci., 15, 905–917, https://doi.org/10.5194/nhess-15-905-2015, 2015.

Sund, M., Grønsten, H. A., and Seljesæter, S. Å.: A regional early warning for slushflow hazard, Nat. Hazards Earth Syst. Sci., 24, 1185–1201, https://doi.org/10.5194/nhess-24-1185-2024, 2024.

Techel, F., Pielmeier, C. and Schneebeli, M.: Microstructural resistance of snow following first wetting, Cold Regions Science and Technology, 65, 382-391, https://doi.org/10.1016/j.coldregions.2010.12.006, 2011.

Zhang, S., Pecoraro, G., Huang, D., Peng, J., Zhang, B. and Calvello, M.: From hydro-meteorological thresholds towards an operational warning model for landslides at regional scale: A real-case application, Engineering Geology, 362, 108542, https://doi.org/10.1016/j.enggeo.2026.108542, 2026.